(5) (a) R. L. Zurfluh, L. L. Durham, V. L. Spain, and J. B. Siddall, *J. Am. Chem. Soc.*, **92**, 425 (1970); (b) R. C. Gueldner, A. C. Thompson, and P. A. Hedin, *J. Org. Chem.*, **37**, 1854 (1972).

(6) W. E. Billups, J. H. Cross, and C. V. Smith, *J. Am. Chem. Soc.*, **95**, 3438 (1973).

(7) (a) G. Stork and J. F. Cohen, *J. Am. Chem. Soc.*, **96**, 5270 (1974); (b) B. M. Trost and D. E. Keely, *J. Org. Chem.*, **40**, 2013 (1975); R. L. Cargill and B. W. Wright, *ibid.*, **40**, 120 (1975); J. H. Babler, *Tetrahedron Lett.*, 2045 (1975); W. A. Ayer and L. M. Browne, *Can. J. Chem.*, **52**, 1352 (1974).

(8) A preliminary account of this work has appeared: P. D. Hobbs and P. D. Magnus, *J. Chem. Soc., Chem. Commun.*, 856 (1974).

(9) A. F. Regan, *Tetrahedron*, **21**, 3801 (1969).

(10) T. Matsui, *Tetrahedron Lett.*, 3761 (1967); A. G. Fallis, *ibid.*, 4573 (1973).

(11) T. Tsuji and K. Ohno, *Tetrahedron Lett.*, 3969 (1965); 2173 (1967); J. F. Young, J. A. Osborn, F. H. Jardine, and G. Wilkinson, *Chem. Commun.*, 131 (1965).

(12) K. Sakai, J. Ide, O. Oda, and N. Nakamura, *Tetrahedron Lett.*, 1287 (1972); K. Sakai and O. Oda, *ibid.*, 75 (1972).

(13) A. Blumann and O. Zeitschel, *Ber.*, **46**, 1191 (1913).

(14) The preparation of pure *trans*-verbanone (**24**) and its conversion into the ether **14** has been described: P. D. Hobbs and P. D. Magnus, *J. Chem. Soc., Perkin Trans. 1*, 2879 (1973).

(15) D. J. Pasto, C. C. Cumbo, and P. Balasubramaniyan, *J. Am. Chem. Soc.*, **88**, 2187 (1966).

(16) J. C. Collins, W. W. Hess, and F. J. Frank, *Tetrahedron Lett.*, 3363 (1968).

(17) T. W. Gibson and W. F. Erman, *J. Am. Chem. Soc.*, **91**, 4771 (1969); G. Cainelli, B. Kamber, J. Keller, M. L. Mihailovic, D. Arigoni, and O. Jeger,

Helv. Chim. Acta, **44**, 518 (1961).

(18) L. M. Berkovitz and P. N. Rylander, *J. Am. Chem. Soc.*, **80**, 6682 (1958); M. E. Wolff, J. F. Kermin, F. F. Owings, B. B. Lewis, and B. Blank, *J. Org. Chem.*, **28**, 2729 (1963).

(19) W. C. Agosta and W. L. Schreiber, *J. Am. Chem. Soc.*, **93**, 3947 (1971).

(20) W. D. Burrows and R. H. Eastman, *J. Am. Chem. Soc.*, **81**, 245 (1959); W. Huckel and E. Gelchscheimer, *Justus Liebigs Ann. Chem.*, **625**, 12 (1959).

(21) T. W. Gibson and W. F. Erman, *J. Am. Chem. Soc.*, **91**, 4771 (1969); A. G. Hartmann and R. E. Youngstrom, *J. Org. Chem.*, **34**, 3392 (1969); N. Bosworth and P. D. Magnus, *J. Chem. Soc., Perkin Trans. 1*, 943 (1972).

(22) F. J. McQuillin and R. B. Yates, *J. Chem. Soc.*, 4273 (1965); H. C. Brown and C. P. Garg, *J. Am. Chem. Soc.*, **86**, 1085 (1964).

(23) D. H. R. Barton, J. M. Beaton, L. E. Geller, and M. M. Pechet, *J. Am. Chem. Soc.*, **82**, 2640 (1960).

(24) G. Zweifel and H. C. Brown, *Org. React.*, **13**, 1 (1963); H. C. Brown, *Tetrahedron*, **12**, 117 (1961).

(25) S. Trippett, *Q. Rev., Chem. Soc.*, **17**, 406 (1963); G. Wittig and M. Schlosser, *Chem. Ber.*, **94**, 1373 (1961).

(26) D. B. Denney and J. Song, *J. Org. Chem.*, **29**, 495 (1964); M. Schlosser, and K. F. Christmann, *Angew. Chem., Int. Ed. Engl.*, **3**, 636 (1964).

(27) Only signals for which diagnostic assignments can be made are mentioned.

(28) The optical purity of (+)-nopinone used for the preparation of **26** was 90%. Rotational data are corrected to 100%.

(29) Comparison with spectral data kindly supplied by Dr. C. A. Henrick (Zoecon) of (±)-grandisol showed them to be identical (ir and NMR).

Experimental and Theoretical Studies of the Barrier to Rotation about the N–Cα and Cα–C′ Bonds (φ and ψ) in Amides and Peptides

A. T. Hagler,*[1a] L. Leiserowitz,[1b] and M. Tuval[1b]

Contribution from the Department of Chemical Physics and Department of Structural Chemistry, Weizmann Institute of Science, Rehovot, Israel. Received February 14, 1975

Abstract: The energetics of rotation about the N–Cα (φ) and Cα–C′ (ψ) bonds of methyl groups in simple amide and peptide systems have been studied by experimental and theoretical methods. X-Ray crystal structure analyses of 12 molecular conformations indicated that the position of the minimum in φ (C′–N–Cα–H) was equal to 180° (i.e., C–H anti to the C′–N bond). In ψ (H–Cα–C′–N) the minimum was found to be 0°, i.e., methyl C–H syn to the C′–N bond, based on analysis of ten molecular structures. Variations from these rotational minima appeared to be induced by crystal forces. In order to better understand these phenomena, ab initio molecular orbital, and empirical force field calculations of the rotational potential surface, and lattice energy calculations of the effect of crystal forces on the conformation were carried out. Minimal basis set molecular orbital calculations as carried out here and by others seem to yield results in disagreement with the experimental observations. When extended basis set calculations were carried out it was found that the calculated rotational potential surface in φ is compatible with the experimental results. The location of the minimum in ψ is still not correct, however, although the barrier was found to be almost negligible (0.1–0.2 kcal/mol vs. ~1 kcal/mol in the minimal basis sets). Lattice energy calculations on N-methylacetamide indicated that the crystal forces were of the same magnitude as those due to the rotational potential, in agreement with the experimental observation from various crystals that these forces seem to affect the intramolecular conformations. The minimized lattice energies at different φ's and ψ's were combined with the rotational potential energies as obtained from the various quantum mechanical methods in order to compare the predicted conformation with that observed. The empirical force field calculations using four previously derived different sets of potential functions (three of which having been obtained from fitting crystal data) all yielded the correct minimum in φ. However, in ψ all potentials predicted a minimum in disagreement with the experimental results as in the case of the quantum mechanical calculations. Thus in ψ, all theoretical methods yield the same result, which seems to be at odds with the experimental observations. The results also indicated that a 12th power repulsion may be too "stiff" when applied to the short intramolecular interactions important in determining rotational potentials.

To date the available experimental and theoretical information concerning the energetics of rotation about the N–Cα (φ) and Cα–C′ (ψ) bonds[2,3] in simple amide and peptide systems has been very scarce, and as a consequence the properties of these rotations have not been sufficiently well understood. These systems are important as they serve as model compounds for the analogous rotations in biologically important oligopeptides and proteins 1. The situation is such that up to now not even the position of the minimum energy conformation of

1
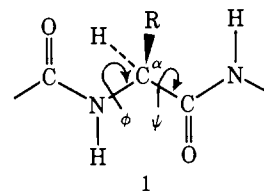
the methyl group in model compounds **2** and **3** has been determined unambiguously. In addition, different theoretical
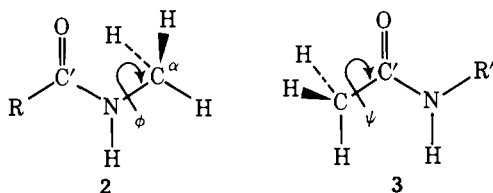
methods have led to different proposed locations for the minima.

In order to obtain a better understanding of these rotations, both experimentally and theoretically, we have undertaken experimental crystal structure analyses of a total of 19 molecules of the types shown in **2** and **3**, as well as quantum mechanical, lattice energy, and empirical force field calculations on a subsample of these.

The apparent differences in the theoretical results for the ϕ torsion are resolved, and the experimental observations are explained in terms of the theoretical results. It is shown that although no theoretical results give the correct position of the barrier in ψ, comparison of extended and minimal basis set results shows that the trend is in the correct direction, and it might be supposed that in the Hartree–Fock limit the calculated barrier would be in the correct position.

In addition to investigating the nature of the rotations in these compounds, another aim of this study is to present a set of objective experimental data on which proposed potential functions for conformational calculations of large biomolecules involving rotations about these angles may be tested. Up to now no objective criteria for rotational potentials about these bonds (ϕ and ψ) have been available and these potentials have had to be constructed from analogy with other compounds[3] (such as ketones, aldehydes, etc.). All molecules considered in this study are given in Figure 1.

Experimental Section

Method. Experimental Determination of Methyl Torsion Angles. The positions of the hydrogen atoms in N-methylacetamide[4] (NMA) and α-chloro-N-methylacetamide,[5] whose structures were previously reported without hydrogens,[4,5] were located by first refining the positional and anisotropic thermal parameters of the C, O, and N (and Cl) atoms with the reported structure factors. This was followed by computation of electron density difference maps on which the hydrogen atoms were evident (Figure 2) and further refinement with isotropic temperature factors for these hydrogen atoms.[6a] (We were not able to locate the hydrogen atoms in the orthorhombic form of acetamide[6b] by these same techniques.)

The methyl torsion angles of all secondary amide structures determined by us were located in a similar manner from the experimentally determined structure factors. The methyl torsions in acetamide in its rhombohedral form[7] and in its complex with barbituric acid,[8a] as well as N-methyldipropylacetamide,[8b] N-acetyl-DL-phenylalanine-N-methylamide,[8c] acetanilide,[8d] and N-acetyl-L-tryptophan methyl ester,[8e] were calculated from the reported hydrogen positions.

The values of the methyl torsion angles as found here are derived from the values of the three individual hydrogen torsion angles (e.g., ϕ_1, ϕ_2, ϕ_3) by taking the average of ϕ_1, $\phi_2 - 120°$, and $\phi_3 - 240°$. It is worth noting in this connection that at room temperature hydrogen atoms are usually not located by x-ray diffraction to the precision required to determined precise molecular geometry (e.g., scatter in bond lengths is often of the order of 0.1 Å and in bond angles as much as 10°, which is an order of magnitude larger than for heavier atoms). However, for our purposes, these deviations are not so serious when the hydrogen positions are used to determine torsion angles for two reasons. The first is that the methyl torsion is determined from *three* hydrogens and thus statistical errors will be reduced by the averaging process. Secondly, the objective in determining torsion angles here is not the precise determination of structure but rather of overall conformation (e.g., the extent of the deviation of the methyl torsion angle from the staggered form). Thus, determination of this angle to within 3–5°, which is attainable by these techniques, is highly satisfactory for our purposes.
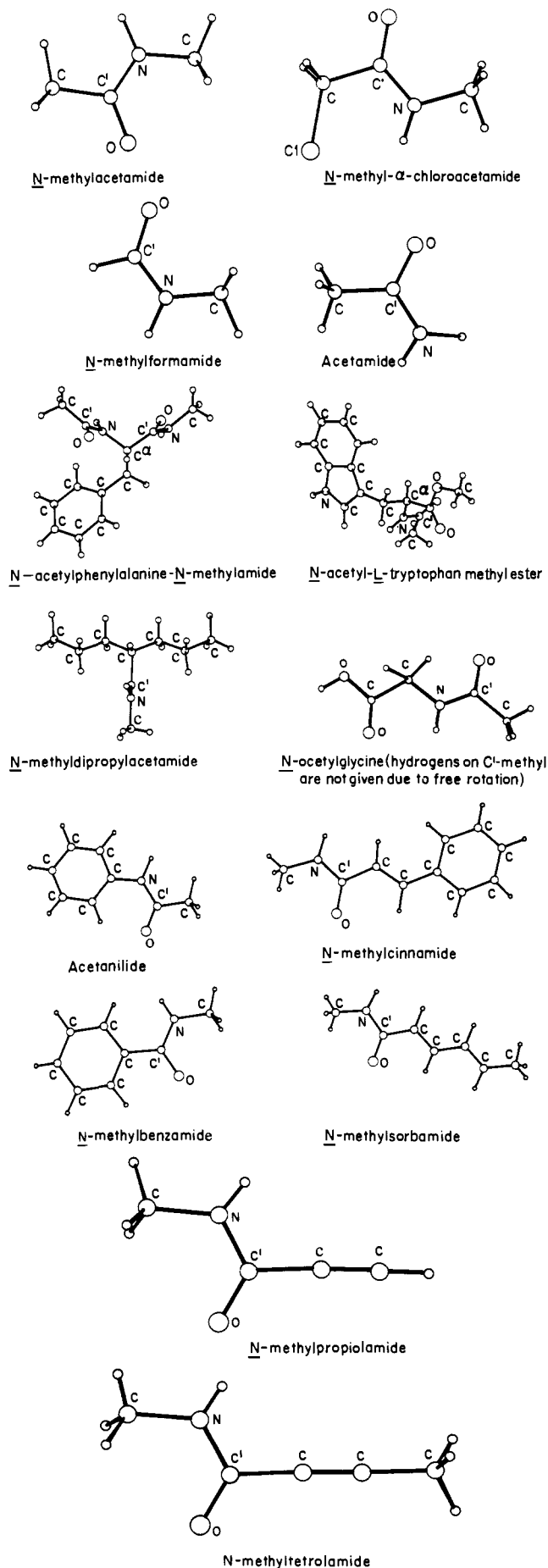

Figure 1. Perspective drawings of all molecules considered in this paper (hydrogen atoms are not labeled).

Table I. Observed Torsion Angles ϕ and ω and Out-of-Plane Angle δ^a in N-Methylamides (Angles in deg)

Molecule	ϕ (H–C$^\alpha$–N–C')	ω (C–C'–N–C)	δ	R (see **2**)
N-Methyltetrolamide[b]	164 (4)[c]	0	0.2	$-C\equiv CCH_3$
N-Methylacetamide[d]	180 (0)[e]	0	0	$-CH_3$
N-Methylpropiolamide[b]	169 (2)	6	5.7	$-C\equiv CH$
N-Methylcinnamide[f]	156 (3)	5	5.8	$-CH=CHC_6H_5$
N-Methylsorbamide[f]	147 (3)	2	1.7	$-C=CHCH=CHCH_3$
N-Methyl-α-chloroacetamide[g]	173 (2)	1	1.1	$-CH_2Cl$
	156 (6)	1	2.3	
N-Methylformamide[h]	125 (7)	4	2.1	$-H$
	118 (6)	2	2.8	
N-Methylbenzamide[f]	167 (2)	1	0.6	$-C_6H_5$
N-Methyldipropylacetamide[i]	179 (7)	0	0.0	$-C(H)(-.CH_2CH_2CH_3)_2$
N-Acetyl-D L-phenylalanine-N-methylamide[j]	144 (12)	5	5.9	

[a] See text for definition of δ. [b] L. Leiserowitz, C. P. Tang, and M. Tuval, to be submitted to *Acta Crystallogr.* [c] The standard deviation in torsion angle as determined from the scatter of the three individual H–C–N–C' torsion angles. [d] Reference 4. [e] The standard deviation of the torsion angle in NMA is zero by virtue of the crystallographic mirror plane. [f] L. Leiserowitz and M. Tuval, to be submitted to *Acta Crystallogr.* [g] Reference 5. [h] Reference 16a. [i] Reference 8b. [j] Reference 8c.
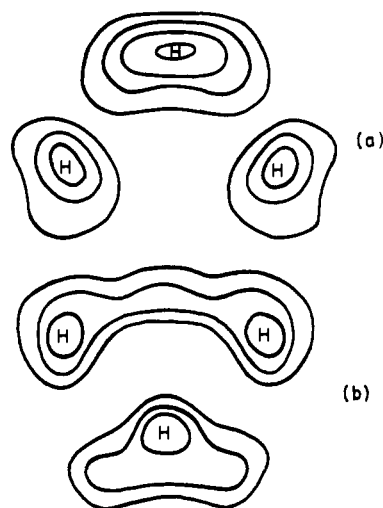

Figure 2. Electron-density difference maps through the plane of the three hydrogens in N-methylacetamide: (a) N-methyl hydrogens; (b) C'-methyl hydrogens.
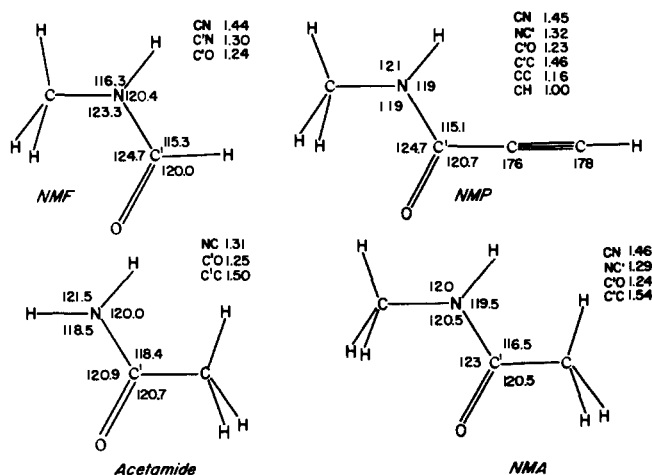

Figure 3. Geometries of N-methylformamide, N-methylacetamide, N-methylpropiolamide, and acetamide used in the calculations carried out in this study. (All methyl groups were taken as tetrahedral with a C–H bond length of 1.11 Å.)

Quantum Mechanical Calculations. We have calculated the torsion barriers in NMA, N-methylformamide (NMF), N-methylpropiolamide (NMP), and acetamide (see Figure 3) using ab initio molecular orbital theory. The energy as a function of the methyl torsion angle at 30° increments was calculated using a minimal Gaussian basis set (STO-3G),[9] and the energy at the minima and maxima of the rotational potentials was also calculated with an extended 6-31G basis set,[10] both sets having been used extensively in studying rotational

barriers.[11] All ab initio calculations were carried out using the "Gaussian-70" program.[12]

Lattice Energy Calculations. We have calculated the effect of crystal lattice energy on the observed methyl torsion angles by varying these angles by 30° and minimizing the lattice energy for each value of the methyl torsion. The minimization is carried out with respect to *all* degrees of freedom of the molecules in the crystal, the only constraint being the number of molecules per unit cell (even crystal symmetry is not imposed).[13a] NMA was chosen for these calculations since it contains both ϕ and ψ rotations and, yet, is still reasonably small.[13b] The initial crystal structures for minimization for those conformations of NMA which contain a mirror plane, i.e., $\phi(120,180)$ $\psi(0,60)$, were generated in the *Pnma* space group, while those which do not contain a mirror plane were generated in the analogous orthorhombic system $Pn2_1a$. The lattice energy for each crystal was calculated with "6-9" and "6-12" potential functions determined previously by fitting the structure and energy of a set of amide crystals as well as the dipole moments of several amide molecules[14] and with a similar set of potential functions ("6-12") reported recently in the literature.[15] The potential functions used are given in Appendix I.

Empirical Force Field Calculations. The rigid rotor rotational potential surfaces for the isolated molecules NMA, NMF, NMP, and acetamide were also calculated by use of the same potential functions discussed above (derived from crystal data and given in Appendix I) by calculating the change in the intramolecular energy at 10° intervals of the appropriate methyl torsion angle. All other geometrical parameters were kept constant and only interactions between atoms separated by three or more bonds were included.

Experimental Results

Variation in ϕ. The values of the torsion angle about the N–CH$_3$ bond (ϕ) for a series of 12 molecules of type **2** contained in ten crystal structures (two of which contain two molecules per asymmetric unit) are given in Table I (along with the values of the out-of-plane angles ω and δ). The torsion angles, ϕ, as given in Table I are such that for conformation **4**, in which one of the C–H bonds is anti to the C'–N bond, ϕ

4
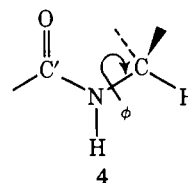
= 180°. (The methyl hydrogen used in defining ϕ is labeled explicitly.) Of these 12 molecules, six exhibit N–CH$_3$ angles (ϕ) close to 180° (i.e., ±15°), four of the torsion angles deviate by as much as 30° from this conformation (e.g., $\phi \simeq 150°$), and only the two molecules of N-methylformamide in the crystal complex of this compound with oxalic acid[16a] exhibit a torsion angle of 120° (i.e., the C'–N bond is eclipsed by a methyl C–H bond[16b]).

Since the N-methyl (N-CH$_3$) is fairly far removed from the R group (see **2**), we would expect that the effect of this group on the intramolecular torsion potential should be small. Therefore it would appear that the differences in conformation observed in Table I are primarily due to the effect of the different intermolecular environments on the N-methyl torsion angle in the different crystals. The crystal structure of N-methyl-α-chloroacetamide[5] (as well as the various acetamides discussed below) provides support for this argument since it contains two molecules per asymmetric unit, which have significantly different ϕ and ψ angles. (Thus the two values of ϕ are 173 and 156°, while the two values of ψ are 179 and 166°).[5] The differences in conformation of the two chemically identical molecules can only be due to the different intermolecular forces, due to the different packing environments.

Comparison with Gas Phase. In this connection it is of interest to compare the conformation of the methyl groups in the gas phase as obtained by recent electron diffraction results with the conformations observed in the crystal. The structure of NMA is of special interest since it is the simplest "peptide" model and various calculations have been carried out on the crystal.[15,17,18] Kitano et al.[19] found that $\phi = 180°$ (as found here in the crystal) gave a significantly better fit to the gas diffraction data than $\phi = 120°$. The fit to the gas diffraction data was insensitive to the conformation of the methyl about the C'–C bond (ψ).

The methyl group in N-methylformamide was also assumed to have one C–H anti to the C'–N bond (i.e., $\phi = 180°$) in the gas phase by Kitano and Kuchitsu;[20] however, this assumption could not be verified as the gas diffraction data were insensitive to this angle.

Variation in ψ. The values of the torsion angles about the C'–CH$_3$ bond (ψ) for ten molecules contained in nine crystal structures are given in Table II. The torsion angles for ψ as given in Table II are such that for comformation **5**, in which

5
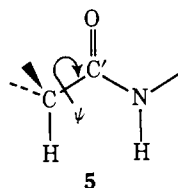
one of the C–H bonds is eclipsed by the C'–N bond, $\psi = 0°$. (The methyl hydrogen used in defining ψ is labeled explicitly.) This set of molecules also bears out that significant differences in the conformation of the methyl group can arise from differences in crystal forces. The same molecule, acetamide, is contained in four different crystal structures and is found to have significantly different values of ψ in the different crystal environments. The inherently favored position of the methyl appears to be $\psi = 0°$ with the largest value of ψ being $\sim 30°$ as found in rhombohedral acetamide.[7]

The situation in N-acetylglycine[21] is of interest in that the methyl group appears to undergo free rotation. In this connection it is noteworthy that the electron diffraction results on diacetamide indicate that one of the C'-methyl groups also exhibits nearly free rotation.[22] Again it would be of interest to compare these results in the crystal with those obtained from gas electron diffraction. Although both acetamide[23] and N-methylacetamide[19] have been studied in the gas phase by this technique, unfortunately the experimental data were insensitive to the location of the methyl group. A more recent study of acetamide and diacetamide[22] by gas diffraction, however, yields a better fit to the data when the methyl group in acetamide is staggered with respect to the C=O bond ($\psi = 0$) in agreement with what is generally found in the crystal. As noted above, one of the methyls in diacetamide was found to be undergoing nearly free rotation, while the other exhibited a

Table II. Observed Torsion Angles ψ in Ten Amides and Peptides

Molecule	ψ (H–C–C'–N)	R' (see 3)
Acetamide[a]	29 (9)	–H
Acetamide[b]	15 (4)	–H
	14 (6)	–H
Acetamide[c]	0 (3)	–H
Acetamide[d]	5 (4)	–H
N-Methylacetamide[e]	0 (0)[j]	–CH$_3$
N-Acetylglycine[f]	Free rotation	–CH$_2$COOH
Acetanilide[g]	13 (b)	–C$_6$H$_5$
N-Acetyl-L-tryptophan[h] methyl ester	1 (7)	
N-Acetyl-DL-phenylalanine-N-methylamide[i]	3 (4)	

[a] Rhombohedral form of acetamide, see ref 7. [b] Acetamide–oxalic acid complex (L. Leiserowitz and F. Nader, to be published). [c] Acetamide–allenedicarboxylic acid complex (L. Leiserowitz and F. Nader, to be published). [d] Acetamide–5,5'-diethylbarbituric acid complex, see ref 8a. [e] Reference 4. [f] Reference 21. [g] Reference 8d. [h] Reference 8e. [i] Reference 8c. [j] See footnote e in Table I.

torsion angle ψ of $\sim 18°$ (± 9)[22] (the differences due, of course, to the folding of the molecule).

Variation in ω. The dihedral angle ω (C$^\alpha$C'NC$^\alpha$) as well as the angle δ between the best plane of the four atoms in the amide group [C$^\alpha$–C(=O)N] and the plane of the three atoms (C'–N–C$^\alpha$) is also included in Table I. The values for ω and δ for these molecules indicate that the deviation from planarity of the amide group is small. A comparison of the trends in ϕ and ω (or δ) shows that there is no apparent correlation between these angles. Of more relevance is the fact that the deviations from planarity which do occur would again seem to be due to intermolecular or crystal forces, as discussed above in the cases of ϕ and ψ. This can be seen by comparing, for example, the analogous molecules of N-methylpropiolamide ($\delta = 5.7°$) with N-methyltetrolamide ($\delta = 0.2°$). Since the only differences in these molecules involve the substitution of a methyl for a hydrogen 4–5 Å removed from the pendant atoms of the C'–N bond (see Figure 1), the effect on the geometry of the amide group should be small (furthermore the deviation from planarity occurs in the propiolamide which contains the hydrogen). A similar situation obtains for the analogous molecules N-methylsorbamide ($\delta = 1.7°$) and N-methylcinnamide ($\delta = 5.8°$).

Qualitative Observations on the Rotational Potential about ϕ and ψ. The results presented above would seem to indicate that both ϕ and ψ have inherently preferred conformations. For ϕ, the minimum appears to be that conformation in which one of the methyl C–H bonds is anti to the C'–N bond, i.e., $\phi = 180°$ as defined here. This is borne out by both the crystal data and the gas diffraction results on N-methylacetamide. The barrier to rotation would appear to be small since it is observed that crystal forces can cause significant variation in the methyl torsion. N-Methylformamide in its crystal complex with oxalic acid presents a unique case in which a methyl C–H bond is found to be syn to the C'–N bond rather than anti. The gas-phase conformation of the methyl in this compound was indeterminate and the conformation in the crystal is probably due to the strong amide–acid packing forces. This phenomenon should provide a nice test of proposed inter- and intramolecular potential functions.

Similar considerations hold for the barrier to rotation about ψ. Here the preferred conformation appears to consist of a methyl C–H syn to the C'–N (i.e., $\psi = 0°$). In this case, however, as indicated by the apparent free rotation of the methyl group in N-acetylglycine in the crystal and in one of the methyl groups in diacetamide in the gas, the barrier to rotation may be very small (e.g., of the order of a few tenths of a kilocalorie).

In order to check these observations quantitatively, both with respect to the approximate size of the rotation barrier, the ef-

Table III. Ab Initio Torsion Potential for ϕ and ψ (STO-3G)

Molecule	ϕ, deg	E, au	$E_\phi - E_{180}$, au	$E_\phi - E_{180}$, kcal
N-Methylformamide	120	-205.25145	-0.00044	-0.28
	150	-205.25123	-0.00022	-0.14
(C'-N, 1.29 A)a	180	-205.25101	0	0
(C'-N, 1.38 A)a	120	-205.26428	-0.00075	-0.47
	150	-205.26389	-0.00036	-0.23
	180	-205.26353	0	0
N-Methylacetamide	120	-243.83660	+0.00005	0.03
($\psi = 0°$)	150	-243.83661	+0.00004	0.02
	180	-243.83665	0	0
N-Methylpropiol-	120	-279.98062	-0.00032	-0.20
amide	150	-279.98046	-0.00016	-0.10
	180	-279.98030	0	0

Molecule	ψ, deg	E, au	$E_\psi - E_0$, au	$E_\psi - E_0$, kcal
N-Methylacetamide	0	-243.83665	0	0
($\phi = 180°$)	30	-243.83739	-0.00074	-0.47
	60	-243.83809	-0.00144	-0.91
Acetamide	0	-205.26034	0	0
	30	-205.26111	-0.00077	-0.48
	60	-205.26187	-0.00153	-0.96

a C'-N = 1.38 corresponds to the gas phase value while C'-N = 1.29 corresponds to the bond distance in the crystal.

Table IV. Barriers to Rotation as Calculated with an Extended Basis Set

Molecule	ϕ, deg	E, au	$E_\phi - E_{180}$, au	$E_\phi - E_{180}$, kcal
N-Methylformamide	120	-207.85776	+0.00052	+0.33
(C'-N, 1.29 A)	180	-207.85828	0	0
(C'-N, 1.38 A)	120	-207.86160	+0.00021	+0.13
	180	-207.86181	0	0
N-Methylacetamide	120	-246.88729	+0.00122	+0.73
($\psi = 0°$)	180	-246.88851	0	0
N-Methylpropiol-	120	-283.50329	+0.00039	+0.25
amide	180	-283.50368	0	0

Molecule	ψ, deg	E, au	$E_\psi - E_0$, au	$E_\psi - E_0$, kcal
N-Methylacetamide	0	-246.88851	0	0
($\phi = 180°$)	60	-246.88860	-0.00009	-0.06
Acetamide	0	-207.88130	0	0
	60	-207.88154	-0.00024	-0.15

Table V. Effect of Geometry on Calculated Rotational Potentials

Molecule	ϕ, deg	E, au	$E_\phi - E_{180}$, au	$E_\phi - E_{180}$, kcal
NMAa	120.0	-243.83700	-0.00057	-0.36
STO-3G	150.0	-243.83670	-0.00028	-0.18
	180.0	-243.83643	0	0
6-31G	120.0	-246.88790	+0.00038	0.25
	180.0	-246.88828	0	0

a NMA with amide geometry of (crystal) NMF.

fect of substituent groups (R), and the magnitude of the effect of the crystal forces, we have carried out ab initio and empirical force-field calculations of the rotation barrier and lattice energy calculations of crystal energy as a function of methyl rotation. These results are presented below.

Results of Ab Initio Calculations

The potential surface for rotation of the methyl groups in N-methylacetamide, N-methylformamide, N-methylpropiolamide, and acetamide as obtained from ab initio calculations with the minimal STO-3G basis set is given in Table III. The barriers to rotation are also calculated with the extended 6-31G basis set and these results are presented in Table IV. The geometries of the molecules used in these calculations are given in Figure 3. Most of the calculations are carried out using the crystal geometry (since our experimental observations are in this phase), although we have also calculated the torsional potential for the gas-phase geometry of NMF to investigate the effects of the significant differences in geometry in the two phases.[20]

As can be seen from Tables III and IV the results of the quantum mechanical calculations are not unequivocal. As expected from the structures of the molecules, the nature of the R group does not make a difference in the location of the barrier although it does seem to affect the barrier height somewhat. The largest difference due to R is approximately 0.5 kcal between the barrier to rotation about ϕ in N-methylacetamide and N-methylpropiolamide in the extended basis set. Although the absolute difference is not large it is of the same order of magnitude as the barrier.

Although the results in Tables III and IV appear to depend on the nature of the R group, analysis of the results of the empirical force field calculations (see Methyl Rotation Barriers section below) indicates that in fact the barrier is very sensitive to the amide geometry (e.g., the OC'N and C'NC angles) rather than to any inductive effect or direct interaction of the N-methyl group with the R group. Thus the OC'N and C'NC angles are slightly smaller in NMA than they are in either NMF or NMP (Figure 3), and it is this difference that leads to the relatively large differences in the barrier heights in these molecules. This is verified and the effect of the geometry (as opposed to inductive and interactive effects) is found by calculating the ϕ rotational potential in NMA with the geometry
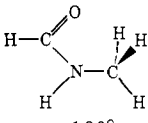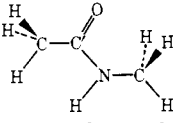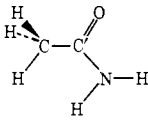
of NMF. These results are given in Table V. Comparison of these results with those for N-methylformamide in Tables III and IV shows that the direct effect of the R group on the barrier is indeed very small ($\sim$0.1 kcal) in both the minimal and extended sets. The variation in geometry either induced by the different R groups or by differences in crystal forces accounts for the rest of the variations in the barrier heights. The reason for this geometric effect and a fuller discussion of it is given in the sections on Methyl Rotation Barriers and Consideration of Deficiencies.

The minimal and extended basis sets, however, do seem to indicate different qualitative behavior independent of the R group or geometry. The minimal basis set results yield a very small barrier in ϕ, with a minimum at $\phi = 120°$, i.e., one of the methyl C-H bonds syn to the C'-N bond contrary to the observed results. The results with the extended 6-31G basis set differ from the smaller basis set by $\sim$0.6-0.7 kcal, and the minimum occurs at $\phi = 180°$ in agreement with the experimental observations (Table I). Again the barrier is very small.

Similar differences exist for ψ. The minimal basis set calculations on acetamide and N-methylacetamide yield barriers of $\sim$1 kcal, which is larger than the calculated barriers for ϕ. Again the location of the minimum as calculated with the minimal basis (a methyl C-H anti to C'-N) is opposite to that we expected from the observations of this angle in the crystal (Table II), i.e., $\psi = 0°$, C-H syn to C'-N. In this case, however, the results obtained with the extended basis seem to produce the same barrier position as the minimal. There is a difference in energy of about 1 kcal between the extended and minimal basis sets favoring the conformation at $\psi = 0°$. However, this is not enough to change the position of the barrier and the result is that the extended calculations still predict a minimum at $\psi = 60°$ although with an extremely small barrier of the order of 0.1-0.2 kcal.

It is of interest to compare these results with those obtained by others, either by the more approximate semiempirical methods or ab initio with different basis sets. These are given in Table VI. The results, for the most part, are very similar to those obtained here with the minimal basis set (Table III).

Table VI. Barriers to Rotation about ϕ and ψ as Calculated by Various Methods

Molecule	Method	ϕ_{min}, deg	ϕ barrier	ψ_{min}, deg	ψ barrier
N-Methylformamide	Ab initio[b] min-Gaussian[a]	180	0.86		
	PCILO[c]	180	0.6		
	CNDO/2[b]	120	0.25		
	EHT[d]	120	0.33		
$\phi = 180°$					
N-Methylacetamide	Ab initio[e] "molecular fragments"	120	0.69	60	1.1
	PCILO[c]	180	0.8	60	1.0
	CNDO/2[d]	120	0.24	60	0.30
	EHT[d]	120	0.30	60	0.18
$\phi = 180°, \psi = 0°$					
Acetamide	Ab initio[b] min-Gaussian[a]			60	1.16
	PCILO[c]			60	0.9
	CNDO/2[d]			60	0.25
	EHT[d]			60	0.21
$\psi = 0°$					

[a] The absolute energies of N-methylformamide (−207.02462) and acetamide (−207.64971) may be compared with those calculated here in Tables III and IV. As seen they are more negative than the STO-3G energies [because more Gaussians were used to describe the inner (1s) orbital]; however, they are less negative than the extended 6-31G energies. [b] See ref 24. [c] See ref 25. [d] See ref 26. [e] See ref 27.

Most of the calculations, with the exception of PCILO[25] and one of the ab initio calculations,[24] give the "wrong" minimum in ϕ of 120° (C–H syn to C'–N). *All* calculations predict a minimum at $\psi = 60°$, most with the rather large barrier of ~1 kcal, contrary to what is expected from the experimental observations. Consideration of the results given above suggests that perhaps the difference in the position of the minimum in ϕ is again due to geometry rather than basis set or method, especially since at least the minimal ab initio basis used[24] is not radically different from the one used here. Indeed the ab initio calculation[24] was carried out with all angles at the C' and N equal to 120°, while the PCILO calculation[25] involved even smaller angles about N (e.g., C'NC = 117°).[28] When the 120° geometry was used with the STO-3G basis used here the minimum in ϕ also was calculated at 180° ($E_{120} - E_{180} \sim 0.4$ kcal), and essentially the same result was obtained with the STO-4G basis. Thus it would seem that these results are again due to the geometry rather than to differences in basis set or method.

It is interesting that the small extended basis set, 6-31G, seems to be the only one used up to now which is able to account for the observed barrier in ϕ with the experimental geometry and, furthermore, is only "slightly" wrong in ψ (see discussion in the section on Methyl Rotation Barriers). It would seem worthwhile to calculate these barriers with still larger basis sets, including polarization functions, to see if the trend continues as one approaches the Hartree–Fock limit.

Lattice Energy and Methyl Rotation

The experimental observations indicate that although the methyl groups have an inherently preferred orientation in ϕ and ψ, this tendency is compromised somewhat by the requirements to optimize the crystal packing energy. It was, in fact, observed that the conformation of the methyl group can vary for the same molecule in different crystal environments. In most cases the deviation from the minimum was less than 30°, but in a few cases this was achieved and even exceeded (Tables I and II). [If the torsion energy is of the form $V_\phi = \frac{1}{2}K_\phi(1 \pm \cos 3\phi)$ a deviation of 30° from the minimum corresponds to an increase of $\frac{1}{2}K_\phi$ or half the barrier height.][29]

In order to further investigate the experimental observations,

which for the most part occur in the crystal phase, and to correlate these with the intrinsic rotational potential as calculated by the various methods, we calculate the effect of the crystal forces on the methyl rotation. In particular we should like to obtain an estimate as to how much the crystal packing energy *at the minimum* changes if the methyl groups are rotated. If this is very large, i.e., much greater than the barrier to rotation, the crystal forces alone will determine the methyl orientation. On the other hand, if the lattice energy is insensitive to methyl rotation, the methyl orientation would be determined solely by the intramolecular "inherently preferred" position. From the experimental observations, we expect that the change in crystal energy with methyl rotation is of approximately the same magnitude as the intramolecular energy (e.g., the barrier height). Thus the calculation of minimum crystal energy changes as a function of methyl rotation should give us corroboratory evidence as to the magnitude of the rotational barrier.

The calculations are carried out on N-methylacetamide,[30] which has the advantage of containing both C'- and N-methyl groups, enabling us to vary both ϕ and ψ, and still being reasonably small.[13b] In addition, it provides a further test of the 6–9 and 6–12 force fields in that it was not one of the molecules used in their derivation[14] (see Appendix II for discussion of fit). For each set of ϕ,ψ, the lattice energy is minimized with respect to *all* crystalline degrees of freedom by methods previously described.[13a] It should be emphasized that the crystal energy *must* be minimized with respect to these variables (i.e., unit cell parameters and molecular orientation) for each structure, since clearly the optimum packing arrangement for one set of methyl orientations need not be the same as for another.

The results of these calculations are given below. The variation in the nonbonded and electrostatic contributions as well as the total lattice energy of NMA as a function of the methyl rotations (ϕ,ψ) are given in Table VII and in the form of contour diagrams in Figure 4a–c. These energies have been calculated with the three force fields, as described in Methods and in Appendix I, in order to avoid conclusions that might be "force field dependent". Comparisons of the calculated and experimental structures of NMA for the 6–9 and 6–12 potentials are given in Figures 5 and 6, and a quantitative sum-

Table VII. Minimized Lattice Energy of N-Methylacetamide as a Function of Methyl Rotations (ϕ and ψ)[a,b]

ϕ,[c] deg	ψ,[c] deg	6–9 potential[e]			6–12 potential[e]			MCMS potential[f]			
		E_{nb}	E_{elec}	E_{lat}	E_{nb}	E_{elec}	E_{lat}	E_{nb}	E_{elec}	E_{hb}	E_{lat}
120	0	−7.97	−7.41	−15.38	−9.92	−6.66	−16.58	−8.36	−1.58	−1.10	−11.04
120	30	−8.38	−7.33	−15.71	−10.17	−6.49	−16.66	−8.71	−1.53	−1.09	−11.33
120	60	−8.70	−7.30	−16.00	−10.76	−6.18	−16.94	−9.12	−1.53	−1.08	−11.73
150	0	−8.00	−7.37	−15.37	−9.79	−6.70	−16.49	−8.30	−1.57	−1.10	−10.97
150	30	−8.33	−7.17	−15.50	−10.16	−6.31	−16.47	−8.48	−1.50	−1.08	−11.06
150	60	−8.80	−7.08	−15.88	−10.75	−6.02	−16.77	−8.92	−1.51	−1.07	−11.50
150	90	−8.43	−7.33	−15.76	−10.42	−6.31	−16.73[d]	−8.76	−1.52	−1.06	−11.34[d]
180	0[b]	−7.90	−7.77	−15.67[b]	−9.97	−6.82	−16.79[b]	−8.66	−1.64	−1.10	−11.40[b]
180	30	−8.50	−7.24	−15.74	−10.38	−6.32	−16.70	−8.71	−1.54	−1.07	−11.32
180	60	−9.03	−6.81	−15.84	−10.87	−5.77	−16.64	−8.85	−1.45	−1.01	−11.31

[a] E_{nb}, E_{elec}, and E_{hb}, are the nonbonded, electrostatic, and hydrogen bonded (in MCMS) contributions to the total lattice energy (E_{lat}), respectively. All energies are in kcal/mol. [b] The experimental conformation consists of ϕ = 180°, ψ = 0°. [c] In cases of symmetry ϕ,ψ (120,30)/(120,90), (150,0)/(−150,0), (150,30)/(−150,90), (150,60)/(−150,60), (150,90)/(−150,30), and (180,30)/(180,90), the second pair is omitted from the table since the energies are identical (see contour maps, Figure 4a–c). [d] The final structure of this conformation was monoclinic rather than orthorhombic (β ~95° for both 6–12 and MCMS potentials). [e] See ref 14. [f] See ref 15.
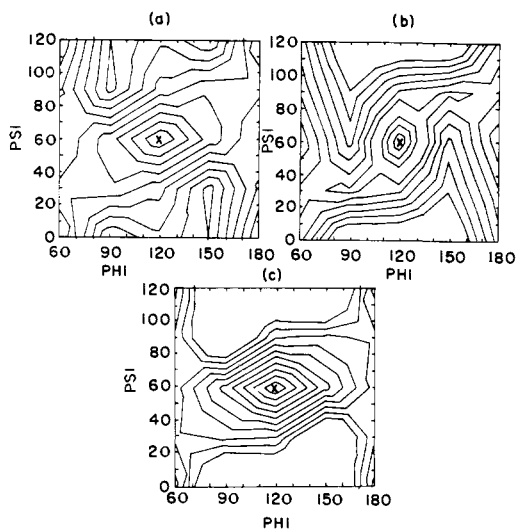

Figure 4. Contour maps of the lattice energy of NMA as a function of rotation of the N-methyl groups about the N–CH₃ bond (ϕ) and the C'–CH₃ bond (ψ) (the contours are spaced at 0.05 kcal/mol intervals and X marks the minimum energy point): (a) 6–12 potential; (b) 6–9 potential; (c) MCMS potential.
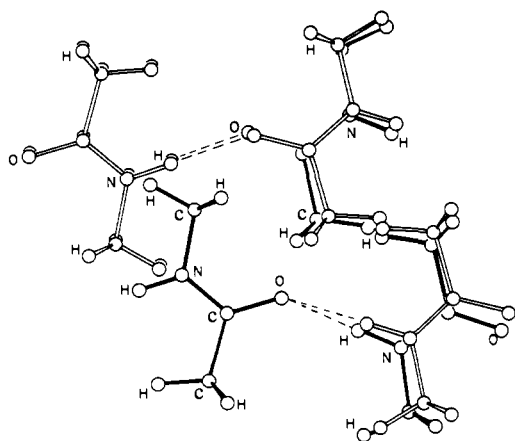

Figure 5. Comparison of the observed and calculated crystal structure of NMA using the 6–9 potential. The observed structure has filled bonds, while the open bonds correspond to the calculated structure. Hydrogen bonds are represented by dashed lines.

Figure 6. Comparison of the observed and calculated crystal structure of NMR using the 6–12 potential. The observed structure has filled bonds, while the open bonds correspond to the calculated structure. Hydrogen bonds are represented by dashed lines.

mary of the fit of these crystals corresponding to those given in ref 14 for all three potentials is given in Appendix II.

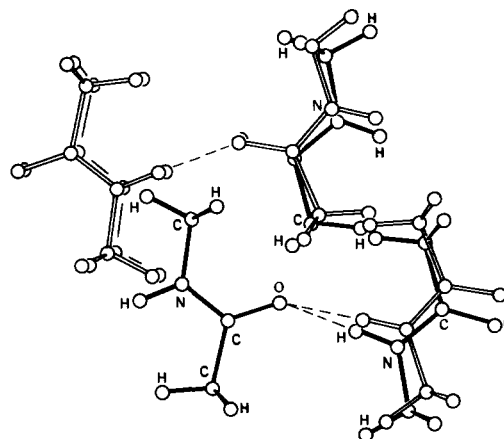The first observation to be made from these calculations is that the difference in packing energies for the various methyl orientations is indeed small. This is true for the energies calculated with all potentials. The largest energy difference is of the order of 0.6–0.7 kcal as calculated with the 6–9[14] and MCMS[15] potentials (corresponding to the difference between the structures ϕ,ψ = (120,60) and (150,0). Thus, if the rotational conformation about ϕ and ψ is to be affected by the requirements of packing, energies of approximately 0.2–0.7 must be commensurate with the magnitude of the rotational potentials. (The cause for the difference in calculated lattice energies between the 6–9 and 6–12 potentials on the one hand and the MCMS potential on the other is discussed in Appendix II.)

The second observation is simply that in no case does the minimum lattice energy correspond to the observed structure. In fact, all potentials give the minimum lattice energy at (120,60) as opposed to the experimentally observed (180,0). There is, of course, no reason why this should not be the case since, as discussed above, the total energy corresponding to the sum of the lattice energy plus rotational energy must be a minimum in the observed crystal.

It is of interest to compare the predicted minimum energy structures as obtained from the lattice energies given above combined with the various rotational potentials obtained from the quantum mechanical methods discussed in the Experimental Results section. These results are presented in Table VIII for the four staggered conformations (ϕ = 120,180; ψ = 0,60). The results for a rotational potential corresponding to that qualitatively predicted from the experimental results as discussed in the Experimental Section with minima at ϕ =

Table VIII. Total Energy (Lattice Plus Rotational) in the N-Methylacetamide Crystal as a Function of ϕ and ψ^a
(All Energies in kcal, $E_{\text{rot}} \equiv 0$ at $\phi = 180°$, $\psi = 0°$)

			Total energy $(E_{\text{lat}} + E_\phi + E_\psi)$							
ϕ, deg	ψ, deg	E_{lat}	Ab initio[b]	Ext[c]	Ab initio[d]	Ab initio[e]	CNDO[f]	EHT[g]	PCILO[h]	Exptl[i]
					(a) 6–9 Potential[k]					
120	0	−15.38	−15.35	−14.65	−14.52	−16.07	−15.52	−15.68	−14.58	−14.65
120	60	−16.00	−16.88[j]	−15.23	−16.30	−17.79[j]	−16.54[j]	−16.48[j]	−16.20	−14.87
180	0[a]	−15.67	−15.67	−15.67	−15.67	−15.67	−15.67	−15.67	−15.67	−15.67[j]
180	60	−15.84	−16.75	−15.90[j]	−17.00[j]	−16.94	−16.14	−16.02	−16.84[j]	−15.54
					(b) 6–12 Potential[k]					
120	0	−16.58	−16.55	−15.85	−15.72	−17.27	−16.82	−16.88	−15.78	−15.85
120	60	−16.94	−17.82[j]	16.27	−17.24	−18.73[j]	−17.48[j]	−17.42[j]	−17.14	−15.81
180	0[a]	−16.79	−16.79	−16.79[j]	−16.79	−16.79	−16.79	−16.79	−16.79	−16.79[j]
180	60	−16.64	−17.55	−16.70	−17.80[j]	−17.74	−16.94	−16.82	−17.64[j]	−16.34
					(c) MCMS Potential[l]					
120	0	−11.04	−11.01	−10.31	−10.18	−11.73	−11.28	−11.34	−10.24	−10.31
120	60	−11.73	−12.61[j]	−11.06	−11.43	−13.52[j]	−12.27[j]	−12.21[j]	−11.93	−10.62
180	0[a]	−11.40	−11.40	−11.40[j]	−11.40	−11.40	−11.40	−11.40	−11.40	−11.40[j]
180	60	−11.31	−12.22	−11.37	−12.47[j]	−12.41	−11.61	−11.49	−12.31[j]	−11.01

[a] Experimentally observed structure corresponds to $(\phi,\psi) = (180,0)$. [b] Ab initio method minimal STO-3G as calculated here (Table III) minima at (180,60). [c] Ab initio extended 6-31G as calculated here (Table IV) minima at (180,60). [d] Ab initio minimal basis[23] (Table VI) minima at (180,60). [e] Ab initio "fragment"[26] (Table VI) minima at (120,60). [f] CNDO[25] (Table VI) minima at (120,60). [g] EHT[25] (Table VI) minima at (120,60). [h] PCILO[24] (Table VI) minima at (180,60). [i] "Experimental" rotational potential (see text) minima at (180,0). [j] Predicted minimum in total energy for a given rotational potential. [k] See ref 13b. [l] See ref 16a.

$180°$, $\psi = 0°$ and small barriers are also included in Table VIII. To make this latter quantitative, the barrier in ϕ is taken as 0.73 kcal (the same as the extended basis set result), while a small arbitrary value of 0.3 is chosen for the barrier in ψ. (The zero of rotational energy is taken at $\phi = 180°$, $\psi = 0°$ and thus the rotational contributions can be either positive or negative depending on the location of the predicted barrier.)

In the case of NMA, it is seen that the qualitative potential predicted from the experimental observations is consistent with the lattice energy calculations in that all three potentials, in combination with this torsion potential, yield the experimentally observed structure as the minimum for NMA. The potential, as derived from the extended basis set calculations, also predicts the correct structure in combination with the "6-12" and MCMS potentials but not in the case of the 6-9 potential because of the ψ dependence (although the difference between the calculated minimum energy structure and the observed is only 0.23 kcal). In no other case is the minimum energy structure predicted correctly, mainly because none of the theoretical rotational potentials give the correct ψ dependence, and the predicted minimum is often $\sim$1 kcal (or more) more stable than the observed structure.

Thus the results seem to generally support the conclusions reached from examination of the experimental torsion angles. Furthermore, and perhaps more importantly, we see that lattice energy calculations can be used to provide independent tests of proposed rotational potentials. As better intermolecular potentials become available, and problems of locating hydrogens are overcome, these tests will become even more rigorous. However, even at this stage differences of as much as a kilocalorie in this context are probably significant (i.e., the error in the difference in lattice energies between two "crystals" which differ only by methyl rotation in the molecule is not as much as 1 kcal, and therefore if the predicted structure is more than 1 kcal more stable than the observed, the rotational potential can be considered to be in error).

Methyl Rotation Barriers as Calculated from Potential Functions Derived from Crystal Data

The barriers to rotation may also be calculated from interatomic empirical functions. It is of interest to calculate these barriers from the potential functions recently derived to fit crystal data[13a,14,15] to see how well energy functions derived from intermolecular interactions can account for the energetics
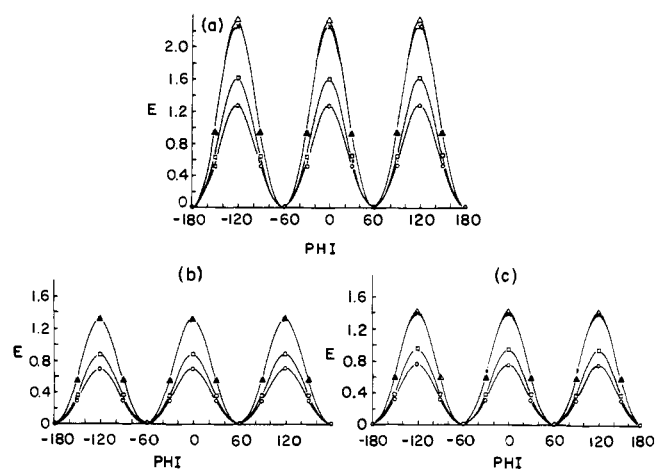

Figure 7. Rotational potential surface in ϕ as calculated with empirical potential functions (see text for details): (a) N-methylacetamide; (b) N-methylformamide; (c) N-methylpropiolamide. Potentials: ×, MCMS; △, 6-12; ○, 6-9; □, BMF.

of these intramolecular rotations. The forms of these functions and the potential constants are given in Appendix I.

These calculations are of special relevance since almost all conformational calculations of peptides and other large molecules of biological interest have been carried out using empirical potential functions.[31,32] The main source of information for the determination of these potential functions is crystal data (structures and sublimation energies) of model compounds. Although this procedure of transferring potential functions determined from crystal data to conformational calculations of large molecules is probably justified for interactions between atoms separated by many bonds, it has been questioned[31] for nearer neighbor interactions such as the 1-4 interactions (atoms separated by three bonds) which are of the utmost importance in determining rotational barriers.

ϕ **Dependence.** The rotational energies as calculated as a function of ϕ, for the potential functions[14,15] used for the lattice energy calculations of the preceeding section, are presented in Figure 7a–c. The empirical potential functions used by Brant et al.[3b] which were derived from other considerations[3b,14] have also been included for comparison. It should be emphasized that only the interatomic pairwise nonbonded and electrostatic

Table IX. Dominant Energy Contributions and Interatomic Distances Affecting Rotational Potential Surface in ϕ^a

Molecule	ϕ	$R_{H\cdots O}$	$E_{nb(H\cdots O)}$	$R_{H\cdots C'}$	$E_{nb(H\cdots C')}$	ΔE^b	Barrier
			BMF Potential^c				
NMA	180	2.72	−0.08	2.70	0.05		
	120	2.26	1.16	2.48	0.64	1.86	1.6
NMF	180	2.82	−0.10	2.73	0.03		
	120	2.37	0.47	2.52	0.49	1.10	0.86
NMP	180	2.81	−0.10	2.74	0.02		
	120	2.35	0.55	0.52	0.47	1.18	0.94
			6–9 Potential^d				
NMA	180	2.72	0.19	2.70	0.12		
	120	2.26	1.86	2.48	0.35	1.59	1.3
NMF	180	2.82	0.11	2.73	0.10		
	120	2.37	1.09	2.52	0.29	0.96	0.69
NMP	180	2.81	0.12	2.74	0.10		
	120	2.35	1.19	2.52	0.29	1.04	0.76
			6–12 Potential^d				
NMA	180	2.72	−0.05	2.70	0.42		
	120	2.26	1.56	2.48	1.80	2.62	2.3
NMF	180	2.82	−0.08	2.73	0.35		
	120	2.37	0.69	2.52	1.45	1.60	1.3
NMP	180	2.81	−0.08	2.74	0.32		
	120	2.35	0.79	2.52	1.42	1.73	1.4
			MCMS Potential^e				
NMA	180	2.72	−0.02	2.70	0.35		
	120	2.26	1.71	2.48	1.52	2.57	2.3
NMF	180	2.82	−0.06	2.73	0.29		
	120	2.37	0.78	2.52	1.23	1.56	1.3
NMP	180	2.81	−0.06	2.74	0.26		
	120	2.35	0.89	2.52	1.20	1.69	1.3

^{a} Angles in degrees, distances in Å, and energies in kcal/mol. $^b \Delta E = (E_{nb(O\cdots H)} + E_{nb(C\cdots H)})_{120} - 2(E_{nb(O\cdots H)} + E_{nb(C\cdots H)})_{180}$. ^{c} See ref 3a. ^{d} See ref 13b. ^{e} See ref 16a.

interactions are included in these curves, and no explicit "cosine type" torsional potentials are imposed. (The threefold maxima, cosine type dependence is seen to arise naturally from these pairwise interactions and the threefold symmetry of the methyl group.) The calculations are carried out for the three molecules NMA, NMF, and NMP.

Inspection of the rotational potential surfaces as calculated by these functions shows that for all cases the minimum occurs at $\phi = 180°$ as expected from the experimental results. This is in contradistinction to the rotational potentials as calculated by the various quantum mechanical methods, where it was seen that the calculated position of the minimum depended on the approximate method and basis set used. The barrier heights however appear to be very sensitive to not only the potential function but also the R group (see, e.g., 2). This latter result appears at first sight anomalous since the R group is too far from the methyl to significantly effect the rotational barrier in these calculations. Considering first the potential dependence (and anticipating the discussion below as to the causes of the NMA result, i.e., the R dependence), we see that the barrier height in ϕ for the BMF potential is ~0.9 kcal, while the 6-9 barriers are slightly smaller (~0.7 kcal). These would seem to be in qualitative agreement with the results given above. The barrier heights as calculated with the 6-12 crystal potentials are of the order of 1.3-1.4 kcal, and this would seem to be a little too large based on the interpretations given above of the experimental data and the effect of crystal packing. The larger barrier in the 6-12 potentials is of course due to the fact that the inverse 12th power repulsion is steeper than the 9th power. Although the BMF potential is also a 6-12 potential, the steepness in this case is compensated for by the smaller "van der Waals" radii (see Appendix I and discussion in ref 14).

Origin of Barrier at $\phi = 120°$. Consideration of the apparently anomalous results for NMA yields both a better understanding of the nature of the barrier to rotation as calculated in this manner and the limitations of calculating rotational

barriers using the "rigid rotor" model (i.e., keeping the geometry of the molecule fixed as the methyl rotates). The rotational barrier at $\phi = 120°$ is due mainly to the strong repulsive interactions between the methyl hydrogen (synplanar to the C') and the carbonyl oxygen ($r_{H\cdots O} \sim 2.3$ Å) and (to a lesser extent) the carbonyl carbon ($r_{C'\cdots H} \sim 2.5$ Å) as shown in 6a. (Compare with the values of r^* as given in Appendix I.)

6a   6b
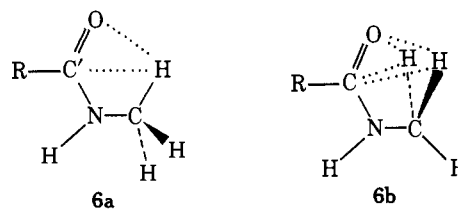
The quantitative values of these interactions for all the molecules and potentials considered here are given in Table IX along with the appropriate distances and the value of the barrier. The latter is compared with the difference in energy of interaction of the methyl hydrogens with the C' and O atoms for $\phi = 120$ and 180° (i.e., those interactions indicated by the dotted lines in 6). It can be seen that most of the barrier to rotation arises from the difference in energy of these interactions. Thus we conclude from these results that, at least from the empirical calculations, *the barrier at $\phi = 120°$ arises from the strongly unfavorable nonbonded contact of a methyl hydrogen with the carbonyl group in this conformation.* This would appear to be a reasonable conclusion, even without any calculations, as the $H_{Me}\cdots O$ distance of 2.3-2.4 Å at $\phi = 120°$, from which the high energy results, is extremely short. Furthermore, at $\phi = 180°$ no correspondingly bad contacts occur. The $H_{Me}\cdots H_N$ contact of ~2.3 Å is short but not exceptionally so.

Rigid Rotor Approximation. The cause for the anomalously large barrier in NMA also becomes apparent by inspection of Table IX. The large barrier in NMA arises not due to any in-

Table X. Dominant Energy Contributions and Interatomic Distances Affecting Rotational Barriers in ψ

Molecule	ψ	$R_{H \cdots O}$	$E_{nb(H \cdots O)}$	$R_{H \cdots N}$	$E_{nb(H \cdots N)}$	ΔE^a	Barrier
BMF Potential							
Acetamide	0	2.72	−0.08	2.50	0.24	0.12	0.38
	60	2.50	0.10	2.73	−0.07		
NMA	0	2.74	−0.09	2.48	0.27	0.17	0.50
	60	2.53	0.06	2.71	−0.07		
6–9 Potential							
Acetamide	0	2.72	0.19	2.50	0.93	0.10	0.39
	60	2.50	0.57	2.73	0.32		
NMA	0	2.74	0.17	2.48	0.99	0.15	0.40
	60	2.53	0.50	2.71	0.34		
6–12 Potential							
Acetamide	0	2.72	−0.05	2.50	1.36	0.52	0.8
	60	2.50	0.20	2.73	0.27		
NMA	0	2.74	−0.06	2.48	1.45	0.60	0.9
	60	2.53	0.15	2.71	0.29		
MCMS Potential							
Acetamide	0	2.72	−0.02	2.50	1.27	0.39^b	1.0
	60	2.50	0.25	2.73	0.32		
NMA	0	2.74	−0.03	2.48	1.37	0.43^b	1.2
	60	2.53	0.20	2.71	0.34		

$^a \Delta E = (E_{nb(H \cdots N)} + 2E_{nb(H \cdots O)})_0 - (2E_{nb(H \cdots N)} + E_{nb(H \cdots O)})_{60}$. ^{b}In the MCMS potential the H-methyl–H-amide interaction at $\psi = 0°$ ($r \sim 2.2$) is also considerably repulsive.

teractions of the N-methyl group with the C'-methyl group (R) but rather due to the fact that at $\phi = 120°$ the $H_{Me} \cdots O$ distance is ~ 0.1 Å shorter in NMA than in NMP or NMF. Because this occurs in the steep repulsive region of the nonbonded potential (see Chart I), this small difference in distance causes

Chart I
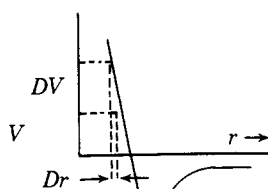
a large difference in energy resulting in the large calculated barrier. The same qualitative behavior was noted in the quantum mechanical results, where the above analysis was anticipated.

Thus the cause of the difference in barrier heights as calculated here is the slight difference in geometry of the amide groups in the three molecules. The smaller $H_{Me} \cdots O$ distance in NMA arises from the fact that both the $C'NC$ and $OC'N$ angles are smaller by a few degrees in NMA than in either NMF or NMP (Figure 3). These results bring out the importance of allowing the geometry to relax (or calculating the barrier for various geometries) since the theoretical results indicate that as the methyl group rotates, small changes in the amide geometry to accommodate it can lead to significant differences in the calculated barrier heights.

ψ **Dependence**. The rotational energies as calculated as a function of ψ for the molecules NMA and acetamide are given in Figure 8 for the potentials discussed above. Here, as with the quantum mechanical calculations, *all* potentials yield a minimum at $\psi = 60°$ (C-H cis to C=O bond) in contradistinction to the conformation expected from the experimental results. Thus we have the unique situation where *all* theoretical methods give the same result, and this result appears to be contrary to the experimental situation.

The calculated barrier heights for NMA and acetamide are essentially the same, smaller than those of ϕ, and, again, as in the case of the ϕ rotation, are considerably different in the
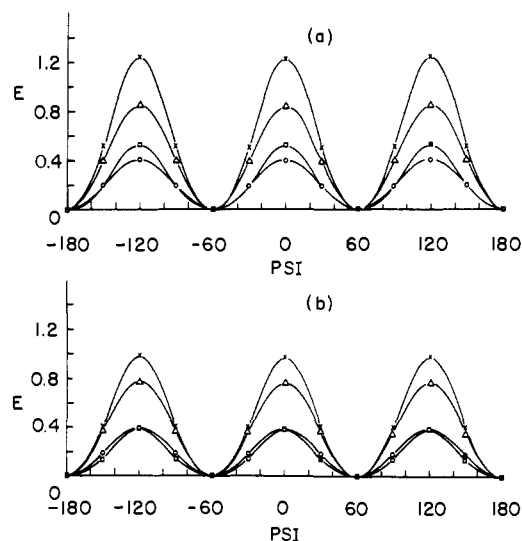

Figure 8. Rotational potential surface in ψ as calculated with empirical potential functions (see text for details): (a) N-methylacetamide; (b) acetamide. Potentials: ×, MCMS; △, 6–12; ○, 6–9; □, BMF.

different potentials. Thus the barrier height as calculated with the BMF and 6–9 potentials is ~ 0.4 kcal, while that calculated with the 6–12 and MCMS potentials is ~ 0.8–1.0 kcal.

The short contacts and their corresponding nonbonded energies are summarized for the two conformations $\psi = 0°$ and $\psi = 60°$ in Table X. The situation is slightly different in the case of the ψ rotation from that in ϕ, in that at both $\psi = 0°$ and $\psi = 60°$ there are considerably unfavorable contacts. In the case of $\psi = 0°$ the $H_{Me} \cdots N$ distance (~ 2.5 Å) is quite short and on the repulsive side of the potential, while for $\psi = 60°$ the $H_{Me} \cdots O$ distance (2.5 Å) is also short. The calculated barrier at 0° arises because of the strongly unfavorable $H \cdots N$ contact which leads to large repulsive energies in all the potentials. The relative small height of the barrier is caused by the fact that the $\psi = 60°$ conformation is also sterically hindered to some extent due to the $H \cdots O$ contact, and the barrier is roughly then the difference between these two positive energies (of course, there are other interactions we have ignored in this discussion, but these are the dominant ones).

Hagler, Leiserowitz, Tuval / Rotational Barrier in Amides and Peptides

Table XI. Nonbonded Parameters and Charges for N-Methylamides[a]

Atom	6–9[d]			6–12[d]			MCMS[e]			BMF[f]		
	$r*$	ϵ	q[b]	$r*$	ϵ	q	$r*$	ϵ	q[b]	$r*$	ϵ	q
H-Methyl	3.54	0.0025	0.11	2.75	0.038	0.10	2.92	0.037	0.025	2.6	0.076	0
O	3.65	0.198	−0.46	3.21	0.228	−0.38	3.12	0.200	−0.387	3.2	0.172	−0.39
N	4.01	0.161	−0.26	3.93	0.167	−0.28	3.99	0.045	−0.344	3.3	0.212	−0.28
C	3.62	0.184		4.35	0.039		4.12	0.038	0.045	3.6	0.138	0
C'	3.75	0.042	+0.46	4.06	0.148	0.38	3.74	0.141	0.465	3.6	0.138	0.39
H-Amide			+0.26			0.28	2.68	0.062[c]	0.164	2.6	0.076	0.28
			(D = 1)			(D = 1)			(D = 2)			(D = 3.5)

[a] The nonbonded potential in eq A1 can also be written as $A/r^n - e/r^6$ where $A_{ii} = 6\epsilon_{ii}r_{ii}*^n/(n - 6)$ and C_{ii} similarly. The cross terms for the 6–9 and 6–12[14] potentials are obtained by $A_{ij} = (A_{ii}A_{jj})^{1/2}$, $C_{ij} = (C_{ii}C_{jj})^{1/2}$. For details as to how the cross terms in the BMF[3b] and MCMS[15] are calculated as well as to the original methods used to derive these parameters, the original references should be consulted. [b] In the 6–9 and 6–12[17] potentials the CH_n group is defined as neutral and the charge on C can therefore be derived from that of H. The charges given for the MCMS potential refer to NMA. The C and H charges given in the table refer to the N-methyl. The charges on the C'-methyl are $q_C = -0.174$ and $q_H = 0.052$. [c] When the amide hydrogen in the MCMS potential is involved in an NH $\cdots$ O hydrogen bond the 6–12 nonbonded interaction is omitted and replaced by the term $12\,040/r_{OH}{}^{12} - 4014/r_{OH}{}^{10}$. [d] See ref 14. [e] See ref 15. [f] See ref 3b.

Table XII. Comparison of Experimental and Calculated Crystal Structures of NMA

	Exptl	Calcd			Molecular	
		6–9 Potential				
a	9.61	9.89 (0.28)	Δx	−0.01	−0.04	0.02
b	6.25	6.36 (−0.16)	Δy	−0.08	−0.08	−0.00
c	7.24	7.19 (−0.5)	Δz	−0.06	0.10	0.18
α	90.0	90.0 (0.0)	θz	0.0	0.0	0
β	90.0	90.0 (0.0)	θx	0.0	0.0	0
γ	90.0	90.0 (0.0)	θy	0.0	−4.6	−4.6
		6–12 Potential				
a	9.61	9.84 (0.23)	Δx	−0.15	−0.32	−0.10
b	6.52	6.26 (−0.26)	Δy	−0.13	−0.13	0.00
c	7.24	7.30 (0.06)	Δz	−0.01	0.22	0.46
α	90.0	90.0 (0.0)	θz	0.0	0.0	0.0
β	90.0	90.0 (0.0)	θx	0.0	0.0	0.0
γ	90.0	90.0 (0.0)	θy	0.0	−7.7	−7.7
		MCMS[a]				
a	9.61	9.97 (0.36)	Δx	−0.02	−0.08	−0.02
b	6.52	6.25 (−0.27)	Δy	−0.13	−0.13	−0.0
c	7.24	7.28 (0.04)	Δz	0.25	0.20	0.66
α	90.0	90.0 (0.0)	θz	0.0	0.0	0.0
β	90.0	90.0 (0.0)	θy	0.0	0.0	0.0
γ	90.0	90.0 (0.0)	θy	0.0	−6.7	−6.7

[a] The results given here differ somewhat from those given in ref 15 since there only three degrees of freedom were allowed (a,b,c) and the orientation of the molecules in the unit cell was kept fixed. In addition, ψ was rotated by 45° from the position used here.

Consideration of Deficiencies in Quantum Basis Functions and Empirical Potential Functions

The comparison of the various theoretical results, both quantum mechanical and empirical, along with a comparison of both with the experimental observations may lead to some conclusions as to the deficiencies in these procedures and possible directions for improvements. The most outstanding result of the calculations is, as mentioned above, that *none* of the theoretical methods gave the correct position for the rotational minima in ψ. The second result which stands out is that *all* the empirical results give the correct position for the minimum in ϕ while in the quantum mechanical methods the position of the minimum depends on basis set. (The importance of geometry is emphasized from the results of both methods.)

It would appear that all of these results may be explained in terms of various degrees of inadequacies in representing the carbonyl oxygen atom. The empirical results suggest that the barrier at $\phi = 120°$ is due to the unfavorable clash between oxygen and methyl hydrogen ($H \cdots O \sim 2.3$ Å). Insofar as this is the only dominant effect (there are essentially no unfavorable interactions at $\phi = 180°$), the empirical calculations predict the location of the minima correctly since they more or less

correctly represent the overall size of the oxygen. This, of course, results from the fact that they were derived by fitting crystal structures, where one of the requirements is that the contact distances be represented correctly. The quantum mechanical calculations, on the other hand, have no "previous information" about the electron density around the carbonyl oxygen, and how well the oxygen is represented depends in part on the validity of the assumptions in the semiempirical methods and to the quality of the basis set in the ab initio calculations[10] (as well as in the semiempirical). The hypothesis that it is the "size" of the carbonyl oxygen which may be the problem is supported by consideration of the minimal (Table III) and extended calculations (Table IV) presented here, where it is seen that the extended basis set (6-31G) correctly predicts the location of the minimum in the potential to be at $\phi = 180°$ while the minimal (STO-3G) gives the wrong position. One indication that electron density about the carbonyl oxygen is more extensive in the extended basis set is that with Mulliken population analysis it is found to have a much larger "charge" (−0.64) in the extended than in the minimal (−0.31). (The extended basis set is known in general to exaggerate charge separation.[10]) Another, more direct indication is that in the cyclic dimer of formamide the calculated N-H $\cdots$ O contact distances are ~ 2.7 Å with the minimal basis set and ~ 3.0 Å with the extended.[33] (The experimental crystal value is ~ 2.9 Å.) Thus the minimal basis set may restrict the electrons to a region too close to the nuclei in the carbonyl oxygen. The greater extension of the electrons in the 6-31G basis set is a natural result of the splitting of the outer orbitals into inner and outer functions in this basis.

The problem with predicting the correct location of the minimum in ψ is more difficult to analyze since as seen from the empirical results, this minimum arises from a set of opposing effects. Here again, however, we suspect the electron distribution of the oxygen may be at fault. The lone-pair orbitals of the oxygen should lie in the plane of the molecule and presumably one of them is directed in the general direction of the methyl hydrogen, increasing the overlap from what it would be for a spherical atom. The problem here may lie in the anisotropy of the electron distribution about the oxygen atom. If this is the case, the empirical potentials, in their present form, cannot cope with this problem since they assume isotropic atoms. Terms would have to be added to account for the effects of anisotropy, as, for example, due to lone-pair orbitals.[14,29,34] These effects should fall out naturally from the quantum mechanical calculations, but here again the basis sets must be complete enough to give good representations of the actual molecular orbitals. It is interesting that although the barriers in ψ at 0° as calculated with minimal basis sets are ~ 1 kcal, those with the extended set are ~ 0.1 and if one "extrapolates"

Table XIII. Average Absolute Differences between Experimental and Calculated Distances ($d < 4$ Å), Hydrogen Bond Distances (r_{OH}), and Angles (N–H $\cdots$ O) and (H $\cdots$ O–C) for N-Methylacetamide

Potential	$|\Delta d|$	$|\Delta r_{OH}|$	$|\Delta\theta_{NHO}|$	$|\Delta\theta_{HOC}|$
6–9	0.10	0.11	0.2	5.7
6–12	0.12	0.08	9.0	0.5
MCMS	0.16	0.09	8.2	15.8

to still more complete sets, it is not unreasonable to expect the barrier to shift to the "correct" position of $\psi = 0°$.

The height of the barriers is, of course, much more difficult to assess from the x-ray results. From the analysis carried out here of the experimental torsion angles, in conjunction with the crystal calculations, it would appear that the barrier heights should be of the order of several tenths of a kilocalorie. The results with the extended basis set in ϕ are in agreement with this assessment. The barriers as calculated with the empirical 6–12 potentials seem to be slightly large and this is attributed to the fact that this potential may be too steep in the short repulsive region. A possible solution to this problem is the use of an exponential repulsive potential[36] which has a more fundamental basis.[37]

A significant number of calculations of rotational potential surfaces of various systems have been carried out, and several mechanisms for decomposing these surfaces into their major components have been proposed.[38] It should be emphasized that by its very nature the above mechanistic discussion is somewhat speculative. Other effects such as bond–bond and attractive interactions for example have been ignored,[39] and there may be other sets of explanations one could produce which could account for the observed effects. We have presented it here since it does seem to be the simplest explanation which is consistent with the whole set of observations and a concrete suggestion for further investigation.

Appendix I

Potential Functions Used for Lattice Energy Calculations and Empirical Rotational Energy Surfaces. The force fields used here to calculate lattice energies and rotational barriers are of the "Lennard-Jones" type.[40] In these force fields the potential energy of interaction between two nonbonded atoms i and j at a distance r_{ij} may be represented by

$$V = \epsilon_{ij}[(6/(n-6))(r^*/r)^n - (n/(n-6))(r^*/r)^6] + q_i q_j / D r_{ij} \quad (A1)$$

where ϵ_{ij} is the depth of the nonbonded potential at the minimum r_{ij}^*, q_i represents the partial charge on atom i, and D is the dielectric constant. The values of the constants in the various nonbonded potentials used here are given in Table XI.

Appendix II

Comparison between Calculated and Observed Crystal Structures of NMA. The experimental and calculated structures of NMA are compared in Tables XII and XIII for the three potentials used in the crystal calculations. The data given correspond to those used in ref 13b (Tables II and III) to analyze the structures of a set of amide crystals.

The structure as calculated with the 6–9 potential is seen to be in best agreement with the observed structure especially with respect to the angular properties of the hydrogen bond. However, all the structures are in reasonable agreement with the observed. As mentioned in the Lattice Energy and Methyl Rotation section, NMA was not one of the molecules used in the derivation of the 6–9 and 6–12 force fields,[14] and thus these results provide a further check on these force fields. A deeper analysis of the structural deviations of the minimized crystal structures from the observed will be presented elsewhere as part

of a study of the crystal structures of secondary amides.

The lattice energy of NMA as calculated with the 6–9 and 6–12 potentials also appears to be in reasonable agreement with experiment. Although the energy of sublimation of NMA has not been measured, the heat of vaporization is ~16.5 kcal/mol[41] and the heat of sublimation should be another 1–3 kcal/mol, in reasonable agreement with the lattice energy of ~16–17 kcal calculated with these potentials. The lattice energy as calculated with the MCMS potential is much lower (−11.4 kcal) due to the small electrostatic contribution. This occurs because the charges in this potential were taken from CNDO/2 and result in a slightly small dipole moment (2.53 vs. ~3.7 experimental)[42] due mainly to the small charge derived for the amide hydrogen. In addition, a dielectric constant of 2 is used in this potential.

References and Notes

(1) (a) Department of Chemical Physics; (b) Department of Structural Chemistry.
(2) For definition of ϕ and ψ see IUPAC, Biochemistry, **9**, 3471 (1970).
(3) (a) H. A. Scheraga, Adv. Phys. Org. Chem., **6**, 103 (1968); (b) D. A. Brant, W. Miller, and P. J. Flory, J. Mol. Biol., **23**, 47 (1967).
(4) J. J. Katz and B. Post, Acta Crystallogr., **13**, 624 (1960).
(5) Y. Koyama, T. Shimanouchi, and Y. Iitaka, Acta Crystallogr., Sect. B, **27**, 940 (1971).
(6) (a) The structure factor least-squares refinement of NMA yielded isotropic temperature factors for the six methyl hydrogens with an average value $U = 0.07$ Å^2 for $\phi = 180°$, $\psi = 0°$. Rotating both methyl groups by 60° resulted in the unacceptable values of 0.18 for the C-methyl group and 0.17 for the N-methyl group. (b) W. C. Hamilton, Acta Crystallogr., **18**, 866 (1965).
(7) W. A. Denne and R. W. H. Small, Acta Crystallogr., Sect. B, **27**, 1094 (1971).
(8) (a) I. N. Hsu and B. M. Craven, Acta Crystallogr., Sect. B, **30**, 974 (1974); (b) C. Cohen-Addad and A. Grand, ibid., **29**, 1149 (1973); (c) I. Harada and Y. Iitaka, ibid., **30**, 1455 (1974); (d) C. J. Brown, Acta Crystallogr., **21**, 442 (1966); (e) M. Cotrait and Y. Barrows, Acta Crystallogr., Sect. B, **30**, 510 (1974).
(9) W. J. Hehre, R. F. Stewart, and J. A. Pople, J. Chem. Phys., **51**, 2657 (1969).
(10) R. Ditchfield, W. J. Hehre, and J. A. Pople, J. Chem. Phys., **54**, 724 (1971).
(11) J. A. Pople, Tetrahedron, **30**, 1605 (1974); (b) J. A. Pople and L. Radom, Jerusalem Symp. Quantum Chem. Biochem., **5**, 747 (1973).
(12) W. J. Hehre, W. A. Lathan, R. Ditchfield, M. W. Newton, and J. A. Pople, Quantum Chemistry Program Exchange, Indiana University, Bloomington, Ind., Program No. 236.
(13) (a) A. T. Hagler and S. Lifson, J. Am. Chem. Soc., **96**, 5327 (1974). (b) Minimization of the energy of one "crystal" (i.e., one set of ϕ and ψ) of NMA with respect to the 27 degrees of freedom[13a,14] takes approximately 8 min on an IBM-370/165. (Energy differences at convergence are $<10^{-4}$ kcal/mol.).
(14) A. T. Hagler, E. Huler, and S. Lifson, J. Am. Chem. Soc., **96**, 5319 (1974).
(15) F. Momany, L. M. Carruthers, R. F. McGuire, and H. A. Scheraga, J. Phys. Chem., **78**, 1595 (1974).
(16) (a) L. Leiserowitz and F. Nader, unpublished results. (b) It should be noted that the intermolecular environment of the two NMF molecules in this complex is very similar.
(17) M. Dentini, P. De Santis, S. Morosetti, and P. Piantanida, Z. Kristallogr., Kristallgeom., Kristallphys., Kristallchem., **136**, 305 (1972).
(18) G. N. Ramachandran, K. P. Sarathy, and A. S. Kolaskar, Z. Naturforsch., A, **28**, 643 (1973).
(19) M. Kitano, T. Fukuyama, and K. Kuchitsu, Bull. Chem. Soc. Jpn., **46**, 384 (1973).
(20) M. Kitano and K. Kuchitsu, Bull. Chem. Soc. Jpn., **47**, 631 (1974).
(21) J. Donohue and R. E. Marsh, Acta Crystallogr., **15**, 941 (1962).
(22) K. L. Gallaher and S. Bauer, private communication.
(23) M. Kitano and K. Kuchitsu, Bull. Chem. Soc. Jpn., **46**, 3048 (1973).
(24) M. Perricaudet and A. Pullman, Int. J. Pept. Protein Res., **5**, 99 (1973).
(25) B. Maigret, B. Pullman, and M. Dreyfus, J. Theor. Biol., **26**, 321 (1970).
(26) Yan, F. Momany, R. Hoffman, and H. A. Scheraga, J. Phys. Chem., **74**, 420 (1970).
(27) L. Shipman and R. E. Christofferson, J. Am. Chem. Soc., **95**, 1408 (1973).
(28) See footnote 81 of ref 27.
(29) Note this commonly assumed form is consistent with the results of the quantum mechanical calculations in that the energies for a 30° rotation are ca. half the calculated barrier heights.
(30) As mentioned above the NMF–oxalic acid complex is also a very appropriate system to calculate since it is unique in that the ϕ torsion in NMF is 120°. This calculation awaits the development of a carboxylic acid force field, which is in progress.
(31) (a) A. T. Hagler and S. Lifson in "The Proteins", 3rd ed, H. Neurath and R. L. Hill, Ed., in press; (b) H. A. Scheraga, Chem. Rev., **71**, 195 (1971).
(32) D. A. Brant, Annu. Rev. Biophys. Bioeng., **1**, 369 (1972).
(33) A. T. Hagler and G. Segal, unpublished results.
(34) Empirical potentials which are used to represent the water molecule have long included the effects of lone-pair orbitals.[35]
(35) (a) A. Duncan and J. Pople, Trans. Faraday Soc., **49**, 217 (1953); (b) A. Ben-Naim and F. H. Stillinger, Jr., in "Water and Aqueous Solutions", R. A. Horne, Ed., Wiley-Interscience, New York, N.Y., 1972, Chapter 8; (c) L. L. Shipman and H. A. Scheraga, J. Phys. Chem., **78**, 909 (1974).

(36) See, e.g., A. I. Kitaigorodskii and K. V. Mirskaya, *Soviet Phys.-Crystallogr.* (*Engl. Transl.*), **9**, 137 (1964).
(37) See, e.g., discussion and references in 31a.
(38) See, e.g., A. Veillard in "Internal Rotation in Molecules", Orville-Thomas, Ed., Wiley, New York, N.Y., 1974, p 385.
(39) See, e.g., N. D. Epiotis, S. Sarkanen, D. Bjorkquist, L. Bjorkquist, and R. Yates, *J. Am. Chem. Soc.*, **96**, 4075 (1974).

(40) In some cases an exponential of the type $A \exp(br_{ij})$ is used instead of the reciprocal *n*th power dependence to describe the nonbonded repulsions (see discussion in ref 28). In addition, explicit terms to represent the hydrogen bond may be included (e.g., ref 15), but these are not involved in any case in the energetics of the methyl rotation.
(41) R. Gopal and S. A. Rizvi, *J. Indian Chem. Soc.*, **45**, 13 (1968).
(42) R. M. Meighan and R. H. Cole, *J. Phys. Chem.*, **68**, 503 (1964).

Structure of a Derivative of Streptovaricin C Triacetate. Crystal and Molecular Structure of the Atropisomer of the Cyclic p-Bromobenzeneboronate Ester of Streptovaricin C Triacetate: Methylene Dichloride 1:1 Solvate

Andrew H.-J. Wang and Iain C. Paul*

Contribution from the W. A. Noyes Chemical Laboratory, School of Chemical Sciences, University of Illinois, Urbana, Illinois 61801. Received October 6, 1975

Abstract: The crystal and molecular structure of a p-bromobenzeneboronate ester of streptovaricin C triacetate has been determined by single-crystal x-ray methods. The derivative studied was of the atropisomer of the naturally occurring form of streptovaricin C triacetate and it crystallized as a 1:1 methylene dichloride solvate. The crystals are orthorhombic, $a = 22.487$ (8), $b = 12.678$ (5), and $c = 19.723$ (6) Å, with four molecules of $C_{52}H_{59}BBrNO_{17} \cdot CH_2Cl_2$ in the space group $P2_12_12_1$. The structure has been refined to an R factor of 0.106 on 2148 nonzero reflections. A strong indication of the absolute configuration was obtained from the x-ray study. The relative configuration, absolute configuration, and conformation of the ansa ring in this derivative of streptovaricin are compared with those found in other derivatives of ansamycins that have been studied by x-rays. Some structural features that may have a bearing on the biological activity of these macrocyclic antibiotics are also described and discussed.

The streptovaricins are a class of antibiotics that contain a naphthoquinone nucleus and a macrocyclic aliphatic ansa bridge, i.e., one connecting two nonadjacent positions in an aromatic nucleus.[1] The streptovaricins, along with the related rifamycins, have been shown to have important biological activity, such as the inhibition of RNA-dependent DNA polymerase (reverse transcriptase) from RNA tumor virus, the inhibition of DNA-dependent RNA polymerase from *Escherichia coli*, and general antiviral and antibacterial properties, especially against mycobacteria.[2] Different members of the streptovaricin class have varying activities in these separate areas of biological action. In particular, the level of acetylation of the several hydroxyl groups in the molecule has a significant effect on activity.

We are planning to undertake a study of the relationship of the detailed three-dimensional structure of molecules of the streptovaricin family to their biological function with the aim of ascertaining some of the factors that govern such activity. As the first step in this direction, we now describe the three-dimensional structure of a p-bromobenzeneboronate ester of streptovaricin C triacetate. This work also served to confirm the earlier chemical work of Rinehart and colleagues as to gross structure[3] and to establish the complete stereochemistry. A preliminary communication has been published.[4] Some more recent studies[5] have shown that the compound studied was in fact the atropisomer of the derivative of streptovaricin C triacetate, rather than the form corresponding to naturally occurring streptovaricin C. Atropisomers in the ansamycins arise due to a reversal of the sense or helicity of the ansa ring (see Figure 1).

Experimental Section

Streptovaricin C triacetate (1) upon reaction with p-bromobenzeneboronic acid gave two derivatives. One of these esters, **2**, was obtained in 16% yield and melted at 215–220°, while the other, **3**, was obtained in 14% yield and melted at 214–217°. The first derivative was originally thought to be an acyclic ester,[4] but the two esters are now recognized to be the two atropisomeric cyclic p-bromobenzeneboronate esters ($C_{52}H_{59}BBrNO_{17}$) of 1 (Figure 1).[5] The helicity of the ansa ring in the ester 2 is now known to correspond to that of naturally occurring streptovaricin C; the x-ray analysis was carried out on a solvate of the atropisomeric ester 3.
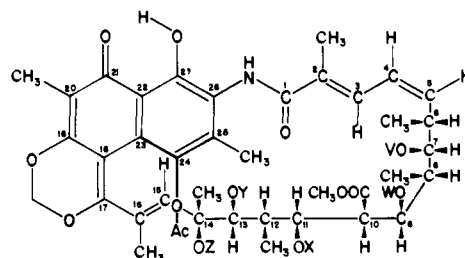
3: V = W = X = Ac, Y + Z = $\rangle BC_6H_4Br(p)$

The ester 3 was crystallized from methylene dichloride–ether to give a methylene dichloride solvate, $C_{52}H_{59}BBrNO_{17} \cdot CH_2Cl_2$ (mp 275–278°), crystals of which were adequate for x-ray structure determination.

Structure Determination of the p-Bromobenzeneboronate Ester of Streptovaricin C Triacetate: Methylene Dichloride 1:1 Solvate. The crystals of the methylene dichloride solvate are red and transparent with a rectangular bar shape, elongated along the *b* axis. A relatively